Multi-Connectivity Resource Allocation with Limited Backhaul Capacity in Evolved LTE

Konstantinos Alexandris, Chia-Yu Chang, Navid Nikaein, Thrasyvoulos Spyropoulos
Communication Systems Department, EURECOM, France
Email: firstname.lastname@eurecom.fr

***Abstract*—Multi-connectivity is considered as a 5G key technique to improve both the user performance and the overall resource utilization. In this paper, we examine a resource allocation problem under multi-connectivity in evolved LTE and propose a utility proportional fair (UPF) resource allocation that preserves users quality-of-service (QoS) considering backhaul capacity limitations. The proposed policy is compared with proportional fair (PF) resource allocation through extensive simulations. Presented results show that multi-connectivity outperforms single-connectivity in terms of network aggregated rate and users QoS satisfaction in different network case studies, i.e., empty and loaded cell scenarios with fixed and variable backhaul capacity.**

***Index Terms*—Multi-connectivity, optimization, utility proportional fairness, Evolved LTE, 5G, backhaul**

I. Introduction

Towards 5G, next generation communication systems are expected to fulfill the insatiable and heterogeneous service requirements. The future network deployments aim to provide ultra-high bandwidth, ubiquitous super-fast connectivity and comprehensive quality-of-service (QoS) in order to meet both network and end-users demands. However, current mobile networks only provide single cell connectivity deployments that set certain bounds on users performance. In single cell connectivity, the user is allowed to be served only from one base station (BS). To overcome such limitation, an approach is to exploit multiple cell connections per end-user perspective on several radio access technologies (RAT) or frequency bands. This approach is usually referred as multi-connectivity [1].

In principle, multi-connectivity targets for effective resource utilization [2], optimized capacity coverage, reliable high-speed data delivery and quick fail-over method support [3]. The dual-connectivity (DC) concept was introduced in LTE Rel.12 study item (3GPP TR36.842) as the simplest case of multi-connectivity enabling two simultaneous connections across the end-users in a single-RAT. Despite its appealing, a significant challenge for multi-connectivity is related to the efficient radio resource utilization [4]. The work in [5] proposes an hierarchical architecture to control and coordinate multi-connectivity with resource allocation and interference management. Further, the authors in [6] consider resource allocation at the macro node side based on DC enabled downlink (DL) connections supported by small cells. Nevertheless, none of these works formally addresses utility-based proportional fairness schemes in a multi-connectivity wireless environment such as to retain users QoS satisfaction.

Further, as the date rate over the air-interface is tremendously increasing, the capacity over the backhaul network is emerged as a major performance bottleneck [7]. In [8], the authors present a distributed power allocation scheme with DC using backhaul state information; however they do not consider any QoS requirement of end-user. In our prior work [9], we examine the benefits of multi-connectivity in terms of user-to-user traffic without considering backhaul non-idealities. To the best of our knowledge, this work is the first one that incorporates both users QoS requirements and network backhaul constraints for the multi-connectivity case. The contributions of our work are summarized as follows:

1) We introduce the system model and assumptions to be used to formulate the utility-based resource allocation problem for *multi-connectivity* in LTE that jointly considers the air-interface limitation and *backhaul* capacity constraints (Section II).
2) Besides fairness among the users, we apply the utility-based resource allocation that takes into account the users *QoS* requirements (Section III).
3) Simulation results show that multi-connectivity is superior to the legacy single-connectivity for different regimes, i.e., empty and loaded cell scenarios with fixed and variable backhaul capacity, in terms of network aggregated rate as well as users QoS satisfaction (Section IV).

Finally, we conclude the paper and present our future plan in Section V.

II. System model

This section describes the system model and the assumptions. We consider a set of BS $\mathcal{B} = \{b_1, \cdots, b_{|\mathcal{B}|}\}$ connected to the core network via backhaul network to serve a set of UE $\mathcal{U} = \{u_1, \cdots, u_{|\mathcal{U}|}\}$. An example is presented in Fig. 1 with $\mathcal{B} = \{b_1, b_2, b_3\}$ and $\mathcal{U} = \{u_1, u_2, u_3, u_4\}$. In Table I, we summarize some applied notations used in this work.[1]

A. Air-interface model

A.1-Carrier frequency: Multi-connectivity deployments are categorized into two different types: (a) Intra-frequency or (b) Inter-frequency. The inter-frequency deployment stands for the case where a UE is multi-connected through different carrier frequencies, either from a single or multi-RAT. While the intra-frequency one refers to transmissions on the same

[1] In addition, bold symbols denote column vectors; $(\cdot)^T$ denotes transpose; $|A|$ denotes the cardinality of a set A.

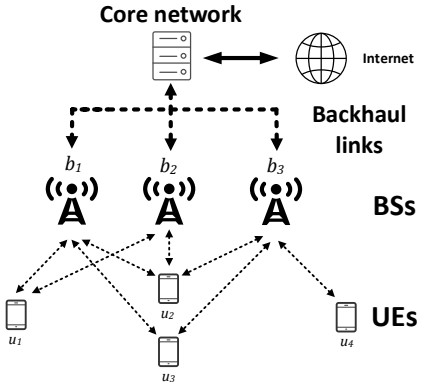

Fig. 1: Multi-connectivity example in LTE network

frequency from a single-RAT, where Coordinated Multipoint (CoMP) schemes are required to mitigate interference [10]. This work applies the inter-frequency single RAT deployment and denotes the DL carrier frequency as f_j^{D} for the j-th BS[2].

A.2-Physical data rate: Each BS b_j can deliver a maximum physical data transmission rate of $R_{j,i}^{\mathrm{D}}$ to a UE u_i (in absence of other served UEs). The physical data rate $R_{j,i}^{\mathrm{D}}$ for the DL in bps is given in Eq. (1) based on the Shannon capacity formula:

$$R_{j,i}^{\mathrm{D}} = B_j^{\mathrm{D}} W_j^{\mathrm{D}} \log_2\left(1 + \mathrm{SINR}_{j,i}^{\mathrm{D}}\right), \tag{1}$$

where B_j^{D} is the j-th BS total number of DL physical resource blocks (PRBs), W_j^{D} is the j-th BS DL bandwidth per PRB in Hz and

$$\mathrm{SINR}_{j,i}^{\mathrm{D}} = \frac{\mathrm{RSRP}_{j,i}^{\mathrm{D}}}{\sum\limits_{b_k \neq b_j,\ f_k^{\mathrm{D}} = f_j^{\mathrm{D}}} \mathrm{RSRP}_{k,i}^{\mathrm{D}} + W_j^{\mathrm{D}} N_0}, \tag{2}$$

is the DL signal-to-interference-plus-noise-ratio (SINR) of the received signal from the j-th BS b_j to the i-th UE u_i. Respectively, the SINR for the UL is denoted as $\mathrm{SINR}_{i,j}^{\mathrm{U}}$.

The DL Reference Signal Received Power (RSRP) $\mathrm{RSRP}_{j,i}^{\mathrm{D}} = L_{j,i}^{\mathrm{D}} P_{j,i}^{\mathrm{D}} G_{j,i}^{\mathrm{D}}$ includes the path loss and shadowing from the j-th BS to the i-th UE $L_{j,i}^{\mathrm{D}}$, the transmission power of the j-th BS to the i-th UE $P_{j,i}^{\mathrm{D}}$, and the combined antenna gain of the j-th BS and the i-th UE $G_{j,i}^{\mathrm{D}}$. The $N_0^{[\mathrm{dBm}]}$ [3] stands for the thermal noise density in dBm per Hz, such that the product $W_j^{\mathrm{D}} N_0$ is the DL aggregated noise power per PRB. Finally, fast fading effects are assumed to be filtered and equalized.

A.3-Uplink Power Control: Open-loop power control is applied along the UL direction and each UE is based on the power control parameters (α, P_0) to compensate the path loss and shadowing effects (i.e., $L_{i,j}^{\mathrm{U}}$). Thus, the transmission power of each PRB from the i-th UE to j-th BS $P_{i,j}^{\mathrm{U[dBm]}}$ in dBm is given as:

$$P_{i,j}^{\mathrm{U[dBm]}} = \min\left(P_i^{\max[\mathrm{dBm}]}, P_0^{[\mathrm{dBm}]} + \alpha \cdot L_{i,j}^{\mathrm{U[dB]}}\right), \tag{3}$$

where $P_i^{\max}$ is the maximum transmission power of the i-th UE that cannot be exceeded. In the DL, the transmission power from the j-th BS to all UEs is the same as $P_{j,i}^{\mathrm{D}} = P_j^{\mathrm{D}}$.

[2] In uplink (UL), notation becomes, e.g., f_j^{U}, while the same holds for the rest of the paper parameters, and is partially skipped for brevity. [3] The notation dBm or dB is skipped when we refer to the linear scale of any quantities.

TABLE I: Parameter notation

Parameter	Description	Direction
$\mathrm{RSRP}_{j,i}^{\mathrm{D\ or\ U}}$	Reference signal received power	DL/UL
$\mathrm{SINR}_{j,i}^{\mathrm{D\ or\ U}}$	Signal to interference plus noise ratio	DL/UL
$\mathrm{SINR}_{\mathrm{th}}$	Signal to interference plus noise ratio threshold	-
$B_j^{\mathrm{D\ or\ U}}$	Total PRB number of j-th BS	DL/UL
$M_i^{\mathrm{D\ or\ U}}$	Maximum PRB number of i-th UE	DL/UL
$W_j^{\mathrm{D\ or\ U}}$	Bandwidth per PRB in Hz	DL/UL
N_0	Thermal noise density	DL/UL
$R_{j,i}^{\mathrm{D\ or\ U}}$	Physical data rate	DL/UL
$\hat{R}_i^{\mathrm{D\ or\ U}}$	Traffic requested rate	DL/UL
$P_{j,i}^{\mathrm{D}}$	DL PRB transmission power of BS	DL
$P_{i,j}^{\mathrm{U}}$	UL PRB transmission power of UE	UL
α, P_0	Open loop power control parameters	UL
$P_i^{\max}$	Maximum transmission power of i-th UE	UL
$C_{h,j}^{\mathrm{D\ or\ U}}$	Backhaul link capacity in bps	DL/UL
$f_j^{\mathrm{D\ or\ U}}$	Carrier frequency in Hz	DL/UL

B. Connection and Traffic model

B.1-Multi-connectivity: In multi-connectivity, UEs can communicate simultaneously with more than one BSs and we assume such multi-connectivity capabilities exist for both DL and UL directions. In specific, a UE can be connected to a BS if both the DL and UL SINR is above a threshold, i.e., $\mathrm{SINR}_{\mathrm{th}}$. Thus, we define the set $\mathcal{E} \triangleq \{(u_i, b_j), (b_j, u_i) : \min\left(\mathrm{SINR}_{i,j}^{\mathrm{U}}, \mathrm{SINR}_{j,i}^{\mathrm{D}}\right) > \mathrm{SINR}_{\mathrm{th}}, \forall b_j \in \mathcal{B}, \forall u_i \in \mathcal{U}\}$ that represents all possible connections. Hence, no connection can be established between the i-th UE and the j-th BS when the condition $\min\left(\mathrm{SINR}_{i,j}^{\mathrm{U}}, \mathrm{SINR}_{j,i}^{\mathrm{D}}\right) > \mathrm{SINR}_{\mathrm{th}}$ does not hold.

B.2-Backhaul network: Backhaul connection can either directly go through wired solution (i.e., star topology) or go through one or more wireless hub cells aggregation points (i.e., tree topology) [11]. In our work, we assume that each BS is connected to the gateway of core network via a dedicated and direct connection (i.e., star topology), see Fig. 1. Finally, we characterize the provisioned capacity of the backhaul link from the j-th BS in both UL and DL as $C_{h,j}^{\mathrm{U}}, C_{h,j}^{\mathrm{D}}$ respectively.

B.3-Traffic requested rate: The UEs are assumed to send and receive traffic from both UL and DL directions. The set of UEs that transmit in UL is defined as $\mathcal{S}$ and the set of UEs receive in DL is defined as $\mathcal{D}$. We denote the user traffic requested rate per direction (UL/DL) as the total rate required by a group of user applications running on the top. This group of user applications can be mapped to bi-directional traffic flows corresponding to the UL and DL while the determined requested rate can reflect the intended user QoS. Specifically, a user u_i sends traffic in the UL by requesting data rate $\hat{R}_i^{\mathrm{U}}$ (UL traffic requested rate) and receives traffic in the DL by requesting data rate $\hat{R}_i^{\mathrm{D}}$ (DL traffic requested rate).

III. Problem Setup

A. Utility function

We define $x_{i,j}^{\mathrm{U}}, x_{j,i}^{\mathrm{D}} \in \mathcal{X}$ as the percentage in decimals on total PRBs allocated by BS b_j to a user u_i to send or receive traffic in UL and DL. In the following, we introduce two different utility functions; one provides proportional fairness and another one extends the proportional fairness by taking into account the users QoS requirements.

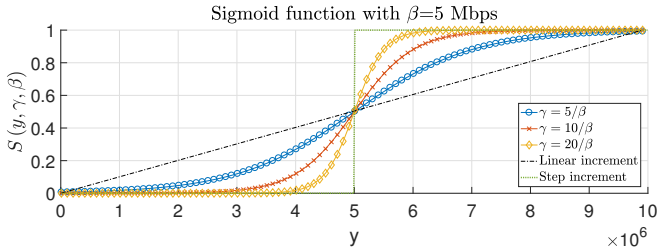

(a) Sigmoid function

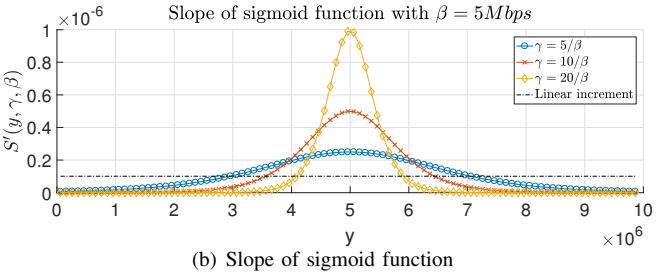

(b) Slope of sigmoid function

Fig. 2: Shape of sigmoid function

1) Proportional Fairness (PF): As the first utility function, we exploit a logarithmic utility function similar to the one in [12] that achieves "proportional fair" resource allocation. The "proportional fair" characteristic implies that if we select a data rate greater than the optimal one, then there will be at least one another data rate that will be decreased in a proportion larger than the proportion of the increased user rate [13]. The utility function is written as

$$\Phi\left(y\right) = \log\left(y\right), \tag{4}$$

where y refers to the allocated data rate.

2) Utility Proportional Fairness (UPF): In the former utility function, a significant drawback lies on the lack of QoS consideration. To incorporate the QoS into the utility function, we use the family of sigmoid functions as:

$$\Phi\left(y\right) = \log\left(S\left(y,\gamma,\beta\right)\right) = \log\left(\frac{1}{1+e^{-\gamma(y-\beta)}}\right), \tag{5}$$

$\gamma > 0$, $y \geq 0$, where β is the traffic requested rate defined as introduced in **B.3** of Section II. The function $\Phi\left(y\right)$ is the natural logarithm of the sigmoid utility function, $S\left(y,\gamma,\beta\right)$, used also in [14] that preserves the traffic requested rate. In Fig. 2(a), the family of sigmoid function with different γ is compared with the linear increment and step increment function for β = 5 Mbps. If the allocated data rate y is less than the requested rate β, the sigmoid function family provides monotonic increment on its slope as shown in Fig. 2(b) whereas its slope is monotonic decreasing when the requested rate is achieved (i.e., $y > \beta$). Moreover, the value of γ impacts the shape of sigmoid function to be more like step or linear function that reflects the demand degree of requested rate.

Based on the aforementioned two utility functions and system model introduced in Section II, we firstly form 4 vectors as $\mathbf{x}_i^{\mathrm{U}} \triangleq \left[x_{i,1}^{\mathrm{U}}, \cdots, x_{i,|\mathcal{B}|}^{\mathrm{U}}\right]^T$, $\mathbf{x}_q^{\mathrm{D}} \triangleq \left[x_{1,q}^{\mathrm{D}}, \cdots, x_{|\mathcal{B}|,q}^{\mathrm{D}}\right]^T$, $\mathbf{R}_i^{\mathrm{U}} \triangleq \left[R_{i,1}^{\mathrm{U}}, \cdots, R_{i,|\mathcal{B}|}^{\mathrm{U}}\right]^T$ and $\mathbf{R}_q^{\mathrm{D}} \triangleq \left[R_{1,q}^{\mathrm{D}}, \cdots, R_{|\mathcal{B}|,q}^{\mathrm{D}}\right]^T$. Then, the per-user utility functions of multi-connectivity proposed for $u_i \in \mathcal{S}$ and $u_q \in \mathcal{D}$ are

$$U_1\left(\mathbf{x}_i^{\mathrm{U}}\right) \triangleq \Phi\left(\left(\mathbf{x}_i^{\mathrm{U}}\right)^T \cdot \mathbf{R}_i^{\mathrm{U}}\right) = \Phi\left(\sum_{b_j \in \mathcal{B}} x_{i,j}^{\mathrm{U}} R_{i,j}^{\mathrm{U}}\right), \tag{6}$$

$$U_2\left(\mathbf{x}_q^{\mathrm{D}}\right) \triangleq \Phi\left(\left(\mathbf{x}_q^{\mathrm{D}}\right)^T \cdot \mathbf{R}_q^{\mathrm{D}}\right) = \Phi\left(\sum_{b_j \in \mathcal{B}} x_{j,q}^{\mathrm{D}} R_{j,q}^{\mathrm{D}}\right). \tag{7}$$

Note $\left(\mathbf{x}_i^{\mathrm{U}}\right)^T \cdot \mathbf{R}_i^{\mathrm{U}}$ and $\left(\mathbf{x}_q^{\mathrm{D}}\right)^T \cdot \mathbf{R}_q^{\mathrm{D}}$ include the aggregated rate over all connected BSs in UL or DL for u_i and u_q and the value of $\hat{R}_i^{\mathrm{U}}$ or $\hat{R}_q^{\mathrm{D}}$ is assigned to β in Eq. (5) for UL or DL.

B. Problem formulation

Based on aforementioned system model, assumptions and utility functions, we then formulate the resource allocation problem. Such problem falls into the category of the network utility maximization for resource allocation and is given as:

$$\begin{aligned}
\max_{\mathcal{X}} \quad & \sum_{u_i \in \mathcal{S}} U_1\left(\mathbf{x}_i^{\mathrm{U}}\right) + \sum_{u_q \in \mathcal{D}} U_2\left(\mathbf{x}_q^{\mathrm{D}}\right) \\
\text{s.t. } \mathbf{C1}: \quad & \sum_{u_i \in \mathcal{S},\, (u_i,b_j) \in \mathcal{E}} x_{i,j}^{\mathrm{U}} \leq 1,\ \forall\ b_j \in \mathcal{B}, \\
\mathbf{C2}: \quad & \sum_{u_q \in \mathcal{D},\, (b_j,u_q) \in \mathcal{E}} x_{j,q}^{\mathrm{D}} \leq 1,\ \forall\ b_j \in \mathcal{B}, \\
\mathbf{C3}: \quad & \sum_{b_j \in \mathcal{B},\, (u_i,b_j) \in \mathcal{E}} x_{i,j}^{\mathrm{U}} B_j^{\mathrm{U}} \leq M_i^{\mathrm{U}},\ \forall\ u_i \in \mathcal{U}, \\
\mathbf{C4}: \quad & \sum_{b_j \in \mathcal{B},\, (b_j,u_q) \in \mathcal{E}} x_{j,q}^{\mathrm{D}} B_j^{\mathrm{D}} \leq M_q^{\mathrm{D}},\ \forall\ u_q \in \mathcal{U}, \\
\mathbf{C5}: \quad & \sum_{b_j \in \mathcal{B},\, (u_i,b_j) \in \mathcal{E}} x_{i,j}^{\mathrm{U}} B_j^{\mathrm{U}} P_{i,j}^{\mathrm{U}} \leq P_i^{\max},\ \forall\ u_i \in \mathcal{U}, \\
\mathbf{C6}: \quad & \sum_{u_i \in \mathcal{S},\, (u_i,b_j) \in \mathcal{E}} x_{i,j}^{\mathrm{U}} R_{i,j}^{\mathrm{U}} \leq C_{h,j}^{\mathrm{U}},\ \forall\ b_j \in \mathcal{B}, \\
\mathbf{C7}: \quad & \sum_{u_q \in \mathcal{D},\, (b_j,u_q) \in \mathcal{E}} x_{j,q}^{\mathrm{D}} R_{j,q}^{\mathrm{D}} \leq C_{h,j}^{\mathrm{D}},\ \forall\ b_j \in \mathcal{B}.
\end{aligned} \tag{8}$$

A detailed explanation of the proposed optimization problem is offered as follows:

Objective function: The objective is to allocate optimally the resources $x_{i,j}^{\mathrm{U}}, x_{j,q}^{\mathrm{D}} \in \mathcal{X}$ for each user $u_i, u_q \in \mathcal{U}$ to maximize the sum of utility functions of all users via applying the per-user utility functions in Eq.(6) and Eq.(7).

Constraints: We elaborate all constraints as following:

- **C1-C2:** These constraints ensure that the number of allocated PRBs (expressed as the percentage in decimals on total PRBs) of each BS b_j to all users shall not exceed the total number of PRBs in both UL and DL directions.
- **C3-C4:** These two constraints assure that the total number of allocated PRBs to each user among all connected BSs will not exceed its maximum number of allocated PRBs, $M_i^{\mathrm{U}}, M_q^{\mathrm{D}}$, in UL and DL, respectively.
- **C5:** Such constraint is related to the power control mechanism in the uplink and it restricts that the total transmission power of the i-th user to all connected BSs can not exceed its power limitations denoted as $P_i^{\max}$.

TABLE II: Simulation parameters

Parameter	Value
LTE mode	FDD, SISO
Frequency band	Band 1 (3×20MHz BW)
Total PRBs of each BS	100 (20 MHz BW)
Maximum PRBs of each UE	100
Number of BSs	3
UE distribution	Uniform for each BS
UE traffic model	Full buffer
SINR threshold	-12 dB
BS transmission power	46 dBm
UE maximum transmission power	23 dBm
Power control parameters	$P_0^{[\text{dBm}]}$ = -58 dBm, $\alpha = 0.8$
Thermal noise density	-174 dBm/Hz
Requested rate distribution	Uniform between 50 to 150 Mbps
γ of UPF utility function	$10/\beta$

- **C6-C7:** These two constraints are related to the backhaul link and they assure that the aggregated rates at each BS b_j will not exceed the provisioned backhaul capacities both in the UL and DL directions.

Finally, the convexity of the proposed problem is proved in the following lemma:

Lemma 1. *The optimization problem proposed in Eq.* (8) *is convex*[4].

Proof. Any of the proposed functions $\Phi(\cdot)$ are strictly concave as the first one is the logarithmic and the second one is the logarithm of the sigmoid function[5]. It is known that any composition of a concave function with an affine function is concave [15]. Thus, we conclude that $U_1\left(\mathbf{x}_i^{\text{U}}\right)$ and $U_2\left(\mathbf{x}_q^{\text{D}}\right)$ are also concave. Consequently, the objective function is concave as a sum of concave functions $U_1\left(\mathbf{x}_i^{\text{U}}\right)$ and $U_2\left(\mathbf{x}_q^{\text{D}}\right)$. Combined with the linear constraints, the problem is convex with an unique tractable optimal solution. □

IV. Simulation Results

In this section, the performance evaluation results are presented for the aforementioned optimization problem. Simulation parameters applied to UEs, BSs and network planning are mostly taken from 3GPP (TR36.814, TR36.942, TR25.942) and NGMN documents, and some important parameters are listed in TABLE II. The whole simulation framework is built in MATLAB and any optimization results are obtained numerically using the interior point method.

Two main simulations scenarios are considered as follows: **Scenario A-Empty cell**: There is 1 BS that serves 0 UEs (i.e., 0% traffic load) while the rest 2 BSs serve non-zero UEs. The empty cell traffic load is used in the evaluation of 3GPP report (TR 25.927) and characterizes some real-world measurement results. We use $0/z/z$ notation to represent this scenario where z is the number of non-zero served UEs per BS. **Scenario B-Loaded cell**: All cells serve non-zero UEs and we use $z/z/z$ notation to represent this scenario. The value of z is 2 or 4 in our simulations. Further, we define two basic metrics: (a) the network aggregated rate as the sum of total allocated rate to all users for DL, $\bar{R}^{\text{D}} \triangleq \sum_{u_q \in \mathcal{D}} \sum_{b_j \in \mathcal{B}} \left(x_{j,q}^{\text{D}}\right)^{\star} R_{j,q}^{\text{D}}$,

[4] Convex solvers such as interior-point methods can be utilized to find the global optimal solutions with great efficiency [15]. [5] The natural logarithm of the sigmoid function is proved as strictly concave in [14].

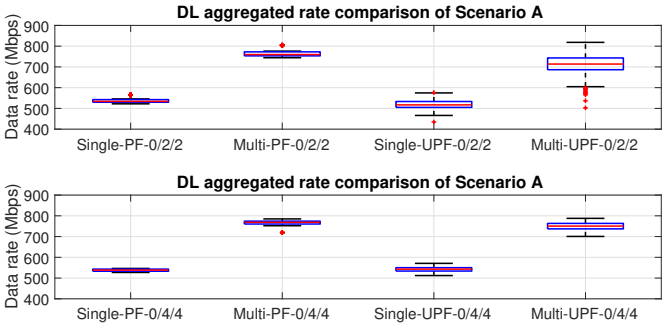

Fig. 3: Aggregated rate of Scenario A

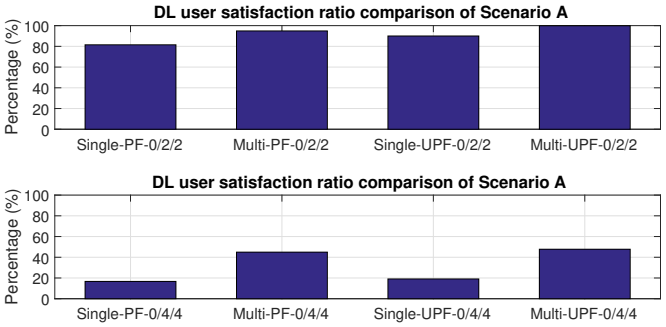

Fig. 4: User satisfaction ratio of Scenario A

where $\left(x_{j,q}^{\text{D}}\right)^{\star}$ are the optimization results in DL (same holds for UL), and (b) the user satisfaction ratio as the percentage of users that are satisfied with the allocated data rate, $S^{\text{D}} \triangleq \text{Prob}\{\sum_{b_j \in \mathcal{B}} \left(x_{j,q}^{\text{D}}\right)^{\star} R_{j,q}^{\text{D}} \geq \hat{R}_q^{\text{D}}\}$ (same holds for UL).

A. Single versus Multi-connectivity

Firstly, we compare the performance of single-connectivity and multi-connectivity under the case of infinite backhaul capacity (i.e., $C_{h,j}^{\text{D}} = C_{h,j}^{\text{U}} = \infty, \forall j$). The considered single-connectivity mode associates each UE to only one BS and only allows each UE to communicate with that associated BS in both UL and DL directions in terms of the best received RSRP. In following, we firstly provide the results of DL direction.

Fig. 3 depicts the aggregated rate of Scenario A under single and multi-connectivity for both PF and UPF case. It can be seen that multi-connectivity outperforms the single one, since it utilizes more resources of the empty cell to enhance the aggregated rate. Additionally, it is noted that PF outperforms UPF as PF aims to boost the aggregated rate while UPF targets to increase the user satisfaction. Further, the same trend is observed in both cases with 2 and 4 UEs per BS, since the applied resource allocation should give the approximately same results in terms of aggregated rate, but not per-user rate as shown in the following user satisfaction results. In Fig. 4, the user satisfaction ratio of Scenario A under single and multi-connectivity for both PF and UPF is shown. Multi-connectivity performs better than the single one as more resources are in use. Further, we notice that UPF is superior to the PF in both single and multi-connectivity (3%-9% gain) for 2 and 4 UEs per BS implying the trade-off between the network aggregated rate and the user satisfaction acquisition. Finally, as the number of users is increasing, the user satisfaction ratio

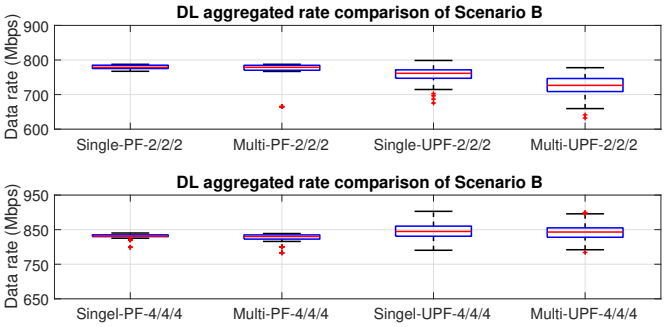

Fig. 5: Aggregated rate of Scenario B

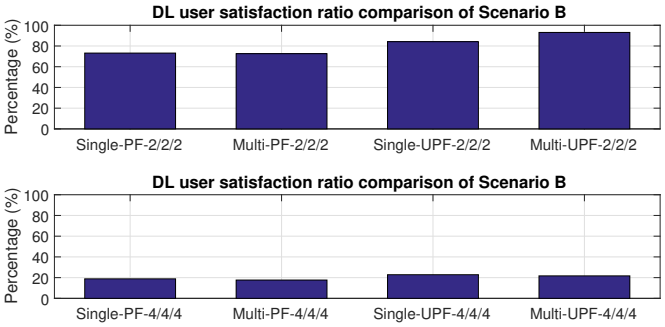

Fig. 6: User satisfaction ratio of Scenario B

is decreasing, since the per-user rate is not sufficient to satisfy the traffic requested rate.

In Fig. 5, we examine analogous results for Scenario B. It is noted that there are no significant differences between single and multi-connectivity as no empty cell resources are available, i.e., loaded cell case. Further, in Fig. 6, we observe that UPF can still increase the user satisfaction when compared to PF in both single and multi-connectivity cases (4%-21% gain) for 2 and 4 UEs per BS. Lastly, the UL resource allocation is similar to the DL ones except for the uplink power control constraint in **C5** of Eq. (8). This constraint further restricts the number of allocated PRBs to each UE and increases the number of unallocated resources at each BS which can be further exploited in multi-connectivity. In that sense, the UL results of Scenario B[6] in Fig. 7 show a higher gain on the aggregate rate and user satisfaction ratio between single and multi-connectivity case when compared with the corresponding gain of DL results in Fig. 5 and Fig. 6.

B. Fixed backhaul capacity limitations

We demonstrate the results for DL with fixed backhaul capacity considering the same value is applied to all backhaul links. In Fig. 8, the average aggregated rate is shown for Scenario A and B with 2 UEs per BS under single and multi-connectivity as a function of the backhaul capacity for both UPF and PF. In both empty and loaded scenarios, the aggregated rate converges when backhaul capacity is provisioned to exceed 300 Mbps in both single and multi-connectivity cases. Regarding Scenario A (i.e., empty cell), it can be seen that multi-connectivity outperforms the single one even with

[6] The UL results for Scenario A show the same behavior with the ones in DL and are omitted due to space limitations.

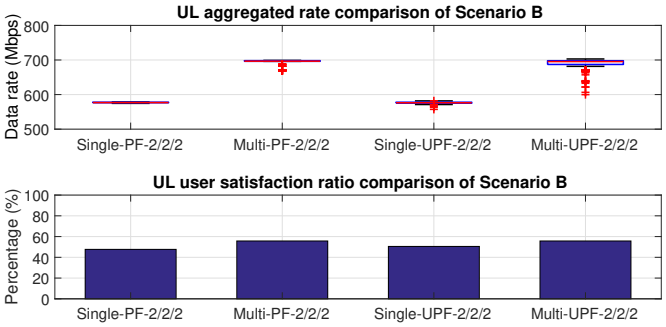

Fig. 7: Uplink result of Scenario B with 2/2/2

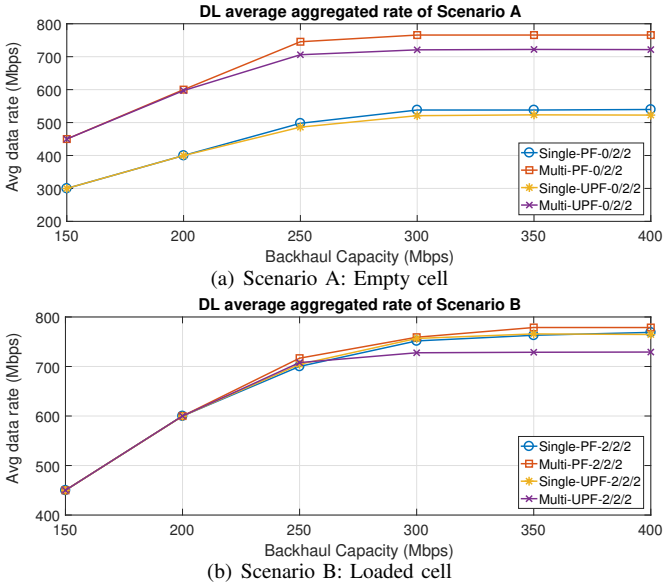

(a) Scenario A: Empty cell

(b) Scenario B: Loaded cell

Fig. 8: Backhaul capacity impact on average aggregate rate

insufficient backhaul capacity, i.e., less than 300 Mbps, via utilizing unallocated backhaul capacity of empty cell. For Scenario B, there are no significant differences between single and multi-connectivity (loaded cell case). Nevertheless, the multi-connectivity case can better reflect the trade-off between achieving higher data rate and attaining higher users satisfaction (i.e., PF versus UPF). In other words, more aggregated rate is sacrificed in multi-connectivity in order to better satisfy the users requested rate when comparing with the single-connectivity case as shown in the following TABLE III.

The user satisfaction ratio results is presented in TABLE III of both Scenario A and B and we observe that the satisfaction ratio can be increased through two manners: (a) apply multi-connectivity (from single to multi-connectivity) where with PF a 3%-31% average gain is observed and with UPF a 7%-34% average gain is offered, and (b) use the UPF utility function (from PF to UPF) where in single connectivity a 7%-10% average gain is inspected while in multi connectivity a 8%-16% average gain is noticed. We highlight that multi-connectivity is beneficial in the empty cell case where it can boost the user satisfaction rate via exploiting more unallocated resources. In addition, UPF can be used to redistribute the network resources based on the users requested rate especially in the loaded cell case when compared with the PF one.

TABLE III: User satisfaction ratio (%) of different BH capacity

Backhaul Capacity (Mbps)	Single PF		Multi PF		Single UPF		Multi UPF	
	0/2/2	2/2/2	0/2/2	2/2/2	0/2/2	2/2/2	0/2/2	2/2/2
150	∼20	∼20	63	∼20	∼20	∼20	81	∼20
200	49	∼50	95	∼50	51	54	100	55
250	72	65	95	68	83	80	100	91
300	81	72	95	73	90	84	100	93
>350	81	72	95	73	90	84	100	93

TABLE IV: Utilization ratio (%) of time-varying BH capacity

Utilization Ratio (%)	Single PF		Multi PF		Single UPF		Multi UPF	
	0/2/2	2/2/2	0/2/2	2/2/2	0/2/2	2/2/2	0/2/2	2/2/2
Air-interface	57	90	94	98	57	90	93	98
Backhaul	63	92	95	93	63	92	93	91

C. Dynamic backhaul capacity limitations

Based on the results of fixed backhaul capacity, we further investigate the time-varying backhaul scenarios (i.e., $C^{\mathrm{D}}_{h,j}(t)$ and $C^{\mathrm{U}}_{h,j}(t)$ are the backhaul capacity at time t). This scenario matches the wireless backhaul condition as introduced in Section II that could be half-duplex in 5G small cell deployment [16]. In Fig. 9(a), we use the time-varying uniformly distributed backhaul capacity between 150 Mbps and 350 Mbps to evaluate the aggregated rate and user satisfaction ratio for both empty and loaded cell scenarios. We observe that multi-connectivity provides a higher aggregated rate for both scenarios (much higher for Scenario A and slightly higher for Scenario B) compared to single one as expected. Further, regarding the user satisfaction ratio results presented in Fig. 9(b), we compare the multi-connectivity to the single one where PF shows a gain of 28% in Scenario A and 5% in Scenario B while UPF offers a gain of 23% in Scenario A and 16% in Scenario B. Finally, respecting the case to compare PF with UPF, in single-connectivity we obtain a gain of 7% for both Scenario A and B while in multi-connectivity we see a gain of 2% for Scenario A and 16% for Scenario B. It can be noticed that the presented results closely lie in the range of gains presented with the finite backhaul capacity representing the anticipated system behavior even with backhaul capacity variability. Table IV summarizes the resource utilization ratio in terms of (a) the percentage of allocated PRBs on air-interface, and (b) the percentage of allocated data rate on backhaul link. Multi-connectivity utilizes better the unallocated resources both in air-interface and backhaul when compared to the single one.

V. Conclusion & Future work

This paper proposes a UPF resource allocation scheme under multi-connectivity considering backhaul constraints that targets to enhance users QoS. Presented results show that multi-connectivity outperforms single-connectivity in terms of: a) network aggregated rate and b) users QoS satisfaction exploiting better the air-interface and backhaul resources in both empty and loaded cell scenarios with fixed and variable backhaul capacity for the PF and UPF respective cases. In future, we plan to introduce more sophisticated techniques as opportunistic scheduling under multi-connectivity regime.

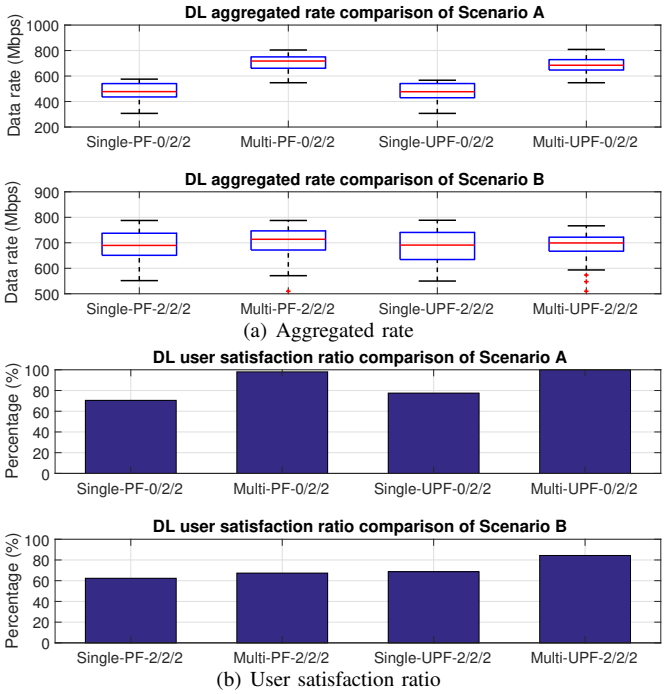

(a) Aggregated rate

(b) User satisfaction ratio

Fig. 9: Time-varying backhaul capacity of both scenarios

Acknowledgments

Research and development leading to these results has received funding from the European Framework Program under H2020 grant agreement 671639 for the COHERENT project.

References

[1] A. Prasad *et al.*, "Enabling RAN moderation and dynamic traffic steering in 5G," in *IEEE VTC-Fall*, 2016, pp. 1–6.

[2] I. Chih-Lin *et al.*, "New paradigm of 5G wireless Internet," *IEEE Journal on Selected Areas in Communications*, 2016.

[3] Nokia, "5G Masterplan - Five keys to create the new communications era," White Paper, 2016.

[4] F. B. Tesema *et al.*, "Mobility modeling and performance evaluation of multi-connectivity in 5G intra-frequency networks," in *IEEE Globecom Workshops*, 2015.

[5] J. Deng *et al.*, "Resource allocation and interference management for opportunistic relaying in integrated mmwave/sub-6 GHz 5G networks," *IEEE Communications Magazine*, 2017.

[6] S. Singh *et al.*, "Proportional fair traffic splitting and aggregation in heterogeneous wireless networks," *IEEE Communications Letters*, 2016.

[7] N. Sapountzis *et al.*, "Optimal downlink and uplink user association in backhaul-limited hetnets," in *IEEE INFOCOM*, 2016.

[8] S. A. Ahmad *et al.*, "Distributed power allocations in heterogeneous networks with dual connectivity using backhaul state information," *IEEE Trans. on Wireless Communications*, 2015.

[9] K. Alexandris *et al.*, "Utility-based resource allocation under multi-connectivity in evolved LTE," in *IEEE VTC Fall*, 2017, pp. 1–6.

[10] M. Shariat *et al.*, "5G radio access above 6 GHz," *Trans. Emerging Telecommunications Technologies*, 2016.

[11] D. L. Oliva *et al.*, "Xhaul: toward an integrated fronthaul/backhaul architecture in 5G networks," *IEEE Wireless Communications*, 2015.

[12] Q. Ye *et al.*, "User association for load balancing in heterogeneous cellular networks," *IEEE Trans. on Wireless Communications*, 2013.

[13] S. Shakkottai *et al.*, "Network optimization and control," *Foundations and Trends in Networking*, 2008.

[14] A. Abdel-Hadi *et al.*, "A utility proportional fairness approach for resource allocation in 4G-LTE," in *IEEE ICNC*, 2014.

[15] S. Boyd *et al.*, *Convex Optimization*. New York, NY, USA: Cambridge University Press, 2004.

[16] U. Siddique *et al.*, "Wireless backhauling of 5G small cells: Challenges and solution approaches," *IEEE Wireless Communications*, 2015.